Cohen Syndrome-Associated Cataract Is Explained by VPS13B Functions in Lens Homeostasis and Is Modified by Additional Genetic Factors

Vincent Lhussiez, Elisabeth Dubus, Quénol Cesar, Niyazi Acar, Emeline F Nandrot, Manuel Simonutti, Isabelle Audo, Eléonore Lizé, Sylvie Nguyen, Audrey Geissler, et al.

Cohen Syndrome-Associated Cataract Is Explained by VPS13B Functions in Lens Homeostasis and Is Modified by Additional Genetic Factors

Vincent Lhussiez,[1] Elisabeth Dubus,[2,3] Quénol Cesar,[2] Niyazi Acar,[3] Emeline F. Nandrot,[2] Manuel Simonutti,[2] Isabelle Audo,[2] Eléonore Lizé,[1] Sylvie Nguyen,[1] Audrey Geissler,[4] André Bouchot,[4] Muhammad Ansar,[5,6] Serge Picaud,[2] Christel Thauvin-Robinet,[1,7,8] Laurence Olivier-Faivre,[1,7,9] Laurence Duplomb,[1,7] and Romain Da Costa[1,7]

[1]INSERM UMR1231, Equipe GAD, Université de Bourgogne Franche Comté, Dijon, France
[2]Sorbonne Université, INSERM, CNRS, Institut de la Vision, Paris, France
[3]Centre des Sciences du Goût et de l'Alimentation, AgroSup Dijon, CNRS, INRAE, Université Bourgogne Franche-Comté, Dijon, France
[4]Plateforme d'Imagerie Cellulaire DImaCell (site CellImaP), INSERM LNC UMR1231, Dijon, France
[5]Institute of Molecular and Clinical Ophthalmology Basel, Basel, Switzerland
[6]Department of Genetic Medicine and Development, University of Geneva Medical School, Geneva, Switzerland
[7]FHU-TRANSLAD, CHU Dijon Bourgogne, Dijon, France
[8]Centre de Référence Déficiences Intellectuelles de Causes Rares, CHU Dijon Bourgogne, Dijon, France
[9]Centre de Référence Anomalies du Développement et Syndromes Malformatifs, CHU Dijon Bourgogne, Dijon, France

Correspondence: Romain Da Costa, INSERM UMR1231, Equipe GAD, Bâtiment B3, 15 boulevard du Maréchal de Lattre de Tassigny, 21089 Dijon, Cedex, France; romain.dacosta@chu-dijon.fr.

Received: June 17, 2020
Accepted: August 14, 2020
Published: September 11, 2020

Citation: Lhussiez V, Dubus E, Cesar Q, et al. Cohen syndrome-associated cataract is explained by VPS13B functions in lens homeostasis and is modified by additional genetic factors. *Invest Ophthalmol Vis Sci.* 2020;61(11):18. https://doi.org/10.1167/iovs.61.11.18

Purpose. Cohen syndrome (CS) is a rare genetic disorder caused by variants of the *VPS13B* gene. CS patients are affected with a severe form of retinal dystrophy, and in several cases cataracts also develop. The purpose of this study was to investigate the mechanisms and risk factors for cataract in CS, as well as to report on cataract surgeries in CS patients.

Methods. To understand how *VPS13B* is associated with visual impairments in CS, we generated the $Vps13b^{\Delta Ex3/\Delta Ex3}$ mouse model. Mice from 1 to 3 months of age were followed by ophthalmoscopy and slit-lamp examinations. Phenotypes were investigated by histology, immunohistochemistry, and western blot. Literature analysis was performed to determine specific characteristic features of cataract in CS and to identify potential genotype–phenotype correlations.

Results. Cataracts rapidly developed in 2-month-old knockout mice and were present in almost all lenses at 3 months. Eye fundi appeared normal until cataract development. Lens immunostaining revealed that cataract formation was associated with the appearance of large vacuoles in the cortical area, epithelial–mesenchymal transition, and fibrosis. In later stages, cataracts became hypermature, leading to profound retinal remodeling due to inflammatory events. Literature analysis showed that CS-related cataracts display specific features compared to other forms of retinitis pigmentosa-related cataracts, and their onset is modified by additional genetic factors. Corroboratively, we were able to isolate a subline of the $Vps13b^{\Delta Ex3/\Delta Ex3}$ model with delayed cataract onset.

Conclusions. VPS13B participates in lens homeostasis, and the CS-related cataract development dynamic is linked to additional genetic factors.

Keywords: Cohen syndrome, VPS13B, ophthalmology, lens, cataract, surgery, inflammation, fibrosis, mouse model, genetic background, genetic modifiers

Cohen syndrome (CS)[1] (OMIM 216550) is a rare autosomal recessive and multisystemic disorder caused by variants of the *VPS13B* gene[2,3] or by copy number variations of its locus on chromosome 8.[4,5] Since its identification, large variability in clinical features associated with the *VPS13B* gene has been described.[6–11] Cardinal manifestations of *VPS13B* mutations are the presence of a typical facial dysmorphism, intellectual disability, intermittent or chronic neutropenia, and progressive retinal dystrophy.[12,13] In most cases, the disease is also characterized by postnatal microcephaly, childhood hypotonia, joint hyperextensibility, abnormal fat distribution, slender extremities, and myopia.[7,14]

Ophthalmic symptoms vary greatly in terms of occurrence, onset, and progression.[15–17] Children suffer from peripheral loss of vision and nyctalopia from a young age. Their electroretinograms are markedly attenuated by the age of 5 and extinguished by the age of 15 years.[16]

Fundus changes in children include the presence of pigment deposits and/or a bull's eye macula.[18] Those two phenotypes are sometimes found associated with optic disc pallor. Deposits usually affect the peripheral retina but can also be observed in the macula of some patients. Studies focusing on ophthalmic phenotypes have also suggested a high prevalence of cataracts in some patient populations with CS, especially in a Greek cohort.[17] Due to potential postoperative complications, cataract management in retinal dystrophies must be carefully considered.[19–21] Although cataract can cause a decrease of visual acuity, about 10% to 15% of retinitis pigmentosa (RP) patients develop cystoid macular edema (CME) after surgery.[22] This feature in patients with very constricted visual fields (<10%), such as CS patients, may cause the visual acuity to worsen. In addition, recent case reports using optical coherence tomography (OCT) suggest that CS patients are more prone to develop CME than RP patients.[23–25] However, in CS patients, cataract can occur very early in adulthood or even in childhood.[17] For this reason, the benefit of cataract surgery is an important question in the medical management of the CS pathology.

While proceeding to the ophthalmic characterization of our recently established *Vps13b*$^{\Delta Ex3/\Delta Ex3}$ mouse model, we identified early-onset forms of hypermature cataracts that cause major retinal inflammation processes. Moreover, we determined that in CS patients, as well as in *Vps13b*$^{\Delta Ex3/\Delta Ex3}$ mice, cataract onset seems to be modified by additional genetic factors. Here, we also report the successful cataract surgery of two CS siblings.

Material and Methods

Animals

The *Vps13b*$^{\Delta Ex3/\Delta Ex3}$ mouse line carrying a constitutive deletion of *Vps13b* exon 3 was established at the Mouse Clinical Institute (MCI)/Institut Clinique de la Souris (ICS) as previously reported.[26] The line was initially produced on a C57Bl/6N background accidently carrying the retinal degeneration-causing mutation *rd8* on the *Crb1* gene. To remove the *rd8* mutation, the *Vps13b*$^{\Delta Ex3/\Delta Ex3}$ line was crossed with wild-type C57Bl6/J mice, and the offspring were genotyped for the *rd8* mutation as previously described.[27] Crossings between *Vps13b*$^{\Delta Ex3/+}$ and *Crb1*$^{rd8/+}$ mice allowed establishment of the *Vps13b*$^{\Delta Ex3/\Delta Ex3}$ *Crb1*$^{+/+}$ C57Bl/6NJ colony used in this study.

Experiments were conducted in accordance with the ARVO Statement for the Use of Animals in Ophthalmic and Vision Research, Federation of European Laboratory Animal Science Associations guidelines for the care and use of laboratory animals (FELASA category B accreditation for R.D.C.), and French legislation (animal quarters agreement nos. C 21-231-008 EA and B 75-12-02 IDV, Théa Pharma), after approval by the local ethics committee (#105, Comité d'Ethique de l'Expérimentation Animale Grand Campus Dijon) and the French Ministry of Higher Education, Research and Innovation (agreement nos. APAFIS#8142-2016121210214682 and APAFIS#9524-2017040712176062). Animals were kept in animal quarters under controlled conditions of temperature (21 ± 1°C) and light (12-hour/12-hour light/dark cycle). Animals were fed ad libitum with standard laboratory chow (SAFE A04; SAFE Complete Care Competence, Rosenberg, Germany) and 0.2-µm filtered water.

Genotyping PCR

Genomic DNA was extracted from tail biopsies through an overnight incubation in lysis buffer (0.2% SDS; 5-mM EDTA; 100-mM Tris, pH8.5; 200-mM NaCl) supplemented with 100-µg/mL Proteinase K (Promega Corp., Madison, WI, USA) at 56°C. The extract was centrifuged at 13,200*g* for 5 minutes following inactivation of Proteinase K at 80°C for 1 hour. A 1:100 dilution of the supernatant was used for genotyping by PCR analysis with GoTaq G2 Flexi DNA Polymerase (Promega) according to the manufacturer's instructions using forward (5′-GCTAGATTGGCTGTCATGAAGCAC) and reverse (5′-CTAACAGTTGACTGAGGAAGCAGCAATG) primers to target a genomic fragment spanning *Vps13b* exon 3 in wild-type mice and including the LoxP sites in knockouts.

Reverse-Transcription and Real-Time Quantitative PCR Analysis

Total RNAs from eye lenses were isolated using Invitrogen TRIzol Reagent (Thermo Fisher Scientific, Waltham, MA, USA) and reverse-transcribed using the iScript Reverse Transcription Supermix (#1708891; Bio-Rad Laboratories, Inc., Hercules, CA, USA) in accordance with the manufacturers' instructions. *Vps13b* mRNA levels were measured by performing real-time quantitative PCR as previously described.[26]

Ophthalmic Examination in Mice

Ophthalmic examination was performed from 1 to 5 months of age on six mice per genotype using the Micron III system (Phoenix Research Laboratories, Pleasanton, CA, USA). The pupils were dilated with tropicamide (Mydriaticum, Théa à l'international Produits, Clermont-Ferrand, France) and phenylephrine (Néosynéphrine; Europhta, Monaco) prior to placing the animals in front of the Micron III device under Isoflurane anesthesia (Axience, Paris, France). During the procedure, eyes were kept moist with 0.9% NaCl. We made use of an excitation filter at 482 nm and an emission filter at 536 nm to detect autofluorescent structures in the retina.

Histology

Vps13b$^{+/+}$ and *Vps13b*$^{\Delta Ex3/\Delta Ex3}$ eyes were collected and fixed in 4% paraformaldehyde for 48 hours and embedded in paraffin. To observe the eye structure, 5-µm-thick sections were stained with Harris hematoxylin and eosin (H&E) Y reagents (Leica Biosystems, Wetzlar, Germany) after paraffin removal. Observations were conducted on an Axioscope microscope (Carl Zeiss Microscopy, Jena, Germany).

Immunofluorescence

Immunostaining was performed on paraffin sections. After paraffin removal, sections were rehydrated and blocked for 30 minutes at room temperature in 1× PBS solution containing 10% fetal calf serum (HyClone; Thermo Fisher Scientific) and 0.3% Triton X-100. Sections were then incubated overnight at 4°C with rabbit primary antibodies diluted in blocking solution, washed in 1× PBS supplemented with 0.1% Tween-20, incubated for 2 hours at room temperature with Donkey anti-Rabbit secondary antibody, Alexa Fluor 568 (#A10042, 1:500; Thermo Fisher Scientific), washed and

mounted in ProLong Diamond Antifade Mountant (#P36961; Thermo Fisher Scientific). Primary antibodies and probes used in this study included anti-GFAP (#GTX108711, 1:200; GeneTex, Inc., Irvine, CA, USA); anti-Iba1 (#AB178846, 1:500; Abcam, Cambridge, UK); anti-α-SMA (#C6198, 1:500; Sigma-Aldrich, St. Louis, MO, USA); anti-Col-IV (#2150-1470, 1:200; Bio-Rad Laboratories); anti-CD4 (#183685, 1:200; Abcam); and ActinGreen 488 ReadyProbes Reagent (#R37110; Thermo Fisher Scientific).

Immunostaining was observed using an AxioVert.A1 microscope (Carl Zeiss Microscopy) equipped with a QImaging Retiga R3 camera (QImaging, Surrey, BC, Canada) and an X-Cite series 120 fluorescence lamp (Excelitas Technologies, Waltham, MA, USA). Images were documented using the Fiji and μManager software packages.

Western Blot Analysis

Retinas were lysed for 20 minutes in 1× radioimmunoprecipitation assay buffer (#9806; Cell Signaling Technology, Danvers, MA, USA) supplemented with 1-mM phenylmethylsulfonyl fluoride and 1× complete protease inhibitor cocktail (#11697498001; Sigma-Aldrich). Cell lysates were centrifuged at 13,000*g* for 20 minutes at 4°C, and protein concentrations were determined using the BCA Protein Assay (Sigma-Aldrich). Proteins were run on sodium dodecyl sulfate–polyacrylamide gel electrophoresis gels and transferred to Millipore Immobilon-P Transfer Membranes (Sigma-Aldrich). Membranes were blotted with antibodies against Phospho-Stat3 (#9145; Cell Signaling); Stat3 (#12640; Cell Signaling); phospho-extracellular signal-regulated kinase 1/2 (Phospho-Erk1/2, #9101; Cell Signaling); Erk1/2 (#4695; Cell Signaling); glial fibrillary acidic protein (GFAP, #GTX108711; GeneTex); ionized calcium-binding adapter molecule 1 (Iba1, #GTX101495; GeneTex); and glyceraldehyde 3-phosphate dehydrogenase (GAPDH, #GTX100118; GeneTex) in 1× PBS, 0.05% Tween-20, and 5% non-fat dried milk. They were then washed and probed with the appropriate secondary antibodies coupled to horseradish peroxidase. Labeled proteins were detected using an enhanced chemiluminescence reagent (Bio-Rad Laboratories) according to the manufacturer's recommendations. Bands were visualized using the ChemiDoc Imaging System (Bio-Rad Laboratories).

Retrospective Literature Analysis

A systematic literature search was performed using the PubMed database to identify relevant studies published between June 2003 (identification of *Vps13b*$^{\Delta Ex3/\Delta Ex3}$ as the disease-causing gene for CS) and April 2020 using the sole key word "Cohen Syndrome." Studies reporting ophthalmic examinations as well as disease-causing variants were included to generate Supplementary Table S1.

Results

Vps13b$^{\Delta ps13bs1.}$ Mice Present with Severe Hypermature Cataracts, Lens Epithelial–Mesenchymal Transition, and Vitreal Fibrosis

To describe the ocular changes affecting *Vps13b*$^{\Delta Ex3/\Delta Ex3}$ mice, ophthalmoscopic examinations were carried out in adult mice. We found that cataract developed as early as 1 month of age in *Vps13b*$^{\Delta Ex3/\Delta Ex3}$ mice and found no fundus alteration before lenses had completely lost transparency (Fig. 1A). Cataract initially appeared as a central loss of transparency (early stages, 1–2 months of age) and evolved within the next weeks or months into complete opacity with vacuolar structures (late stages, 3–5 months of age). Heterozygous *Vps13b*$^{\Delta Ex3/+}$ mice did not show any ophthalmic changes during the course of examination.

We determined the frequency and pace of cataract progression by slit-lamp examination of 1-, 2-, and 3-month-old *Vps13b*$^{\Delta Ex3/\Delta Ex3}$ mice. Cataract affected only about 6% of 1-month-old knockout mice and did so in a bilateral manner for only 2% of animals. Cataract mostly developed within the second month of life, with 33% of 2-month-old mice displaying bilateral cataracts and 21% displaying unilateral cataracts. At the age of 3 months, 92% of knockout mice were affected, of which 77% were so in a bilateral manner (Fig. 1B). In addition, in 2-month-old knockout mice only 37% of cataractous eyes showed complete opacity, but the opacity rapidly progressed to 87% in 3-month-old animals (Fig. 1C). Dissections of eyes with late-stage cataracts (complete opacity) revealed that cataracts had become hypermature, with a complete dissociation of both cortical and nuclear areas of the lens (Fig. 1D). In some eyes, dissociated lens fragments were observable in vivo in the anterior chamber (Fig. 1E).

Histological analysis of early-stage cataracts in *Vps13b*$^{\Delta Ex3/\Delta Ex3}$ mice revealed that cataract formation was initiated after the appearance of large vacuoles in the lens cortical area (Fig. 2A, Supplementary Fig. S1). F-Actin staining revealed that fiber cells had lost the elongated structure that is characteristic of their proper differentiation (Fig. 2B). In later stages, lens dystrophy progressed to an hypermature cataract (HC) aspect through the rupture of the posterior (Fig. 2A) or anterior lens envelope. H&E stainings revealed the abnormal presence of cells in the vitreous humor (Supplementary Fig. S1). We performed immunostaining against α-smooth muscle actin (α-SMA), a common mesenchymal cell marker, and detected α-SMA^{+} cells around the ruptured lens envelope of *Vps13b*$^{\Delta Ex3/\Delta Ex3}$ eyes (Figs. 3A, 3B). Mesenchymal cells are known to be derived from the lens epithelium in response to injuries caused by cataracts.[28] Epithelial–mesenchymal transition (EMT) was also observed in localized areas of the anterior segment of cataractous *Vps13b*$^{\Delta Ex3/\Delta Ex3}$ lenses (Fig. 3C). Immunostaining targeting collagen IV revealed that EMT associated with fibrosis took place in injured *Vps13b*$^{\Delta Ex3/\Delta Ex3}$ lenses (Figs. 3A–3C).

Hypermature Cataract Associates with Infiltration of Immune Cells in the Vitreous Humor and the Retina

We hypothesized that the release of lens material in the vitreous humor may cause the infiltration of immune cells to this compartment and subsequently trigger inflammatory and proliferative responses in retinas of eyes with HC. To confirm the presence of immune cells in the vitreous, we stained *Vps13b*$^{\Delta Ex3/\Delta Ex3}$ eyes with the lymphocyte marker CD4 (Figs. 3D–3F) and confirmed leukocyte infiltration in the vitreous humor of *Vps13b*$^{\Delta Ex3/\Delta Ex3}$ eyes with HC.

Although the retinas of wild-type and cataract-free *Vps13b*$^{\Delta Ex3/\Delta Ex3}$ eyes did not present any abnormalities,

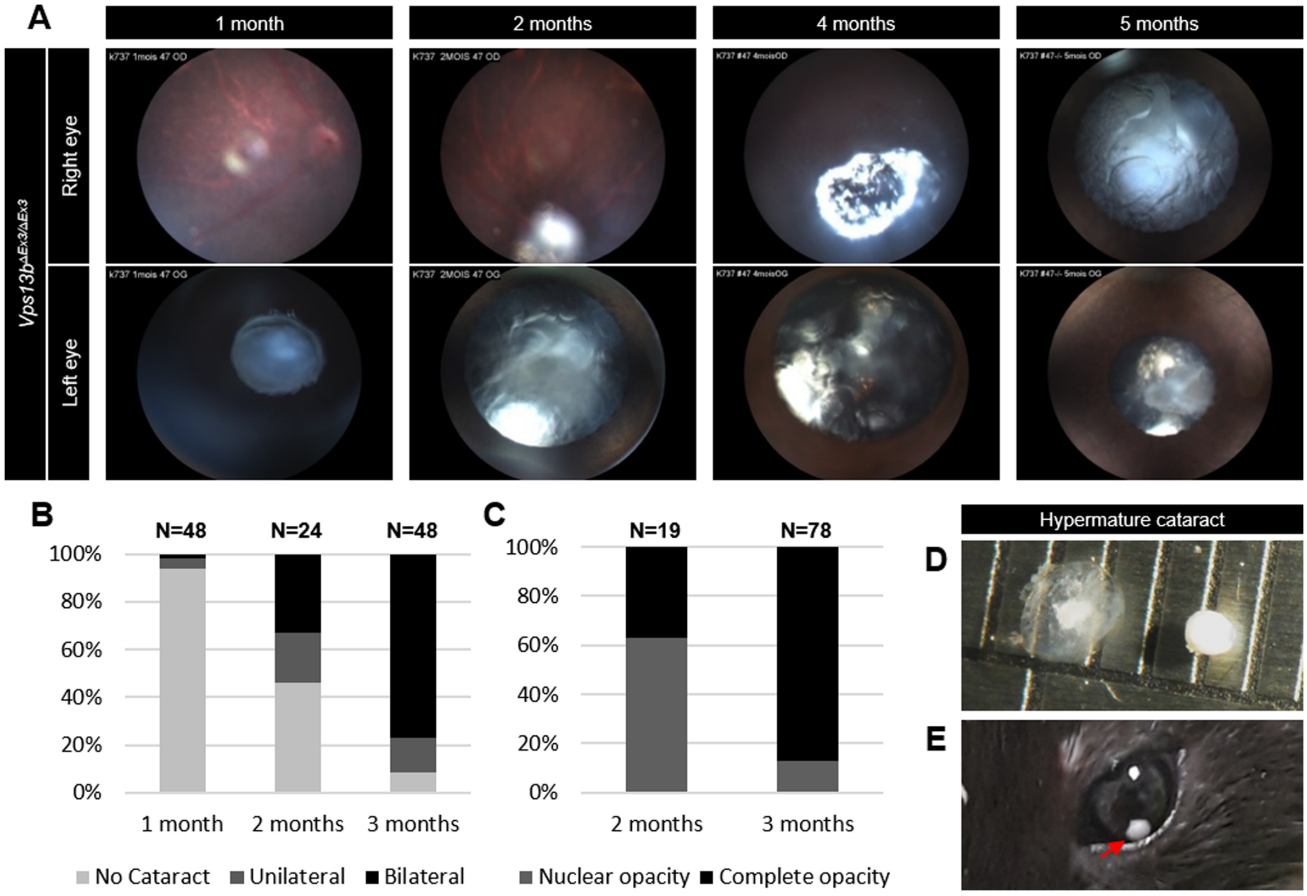

Figure 1. Frequency, characteristics, and progression of cataract in *Vps13b*$^{\Delta Ex3/\Delta Ex3}$ mice. (**A**) Ophthalmoscopic images of *Vps13b*$^{\Delta Ex3/\Delta Ex3}$ eyes displaying the evolution of cataract from 1 to 5 months of age. Note the loss of pupillary response as cataract progresses. (**B**) Frequency of unilateral and bilateral cataracts in 1-, 2-, and 3-month-old knockout mice. Cataracts most frequently appeared between 1 and 2 months of age either uni- or bilaterally. Most 3-month-old knockout mice suffered from bilateral cataracts. (**C**) In order to rank cataract severity, affected eyes were split into two groups depending on whether they showed nuclear opacity only or complete opacity of the lens. Although the majority of affected eyes had only nuclear opacity at 2 months of age, most affected eyes had complete opacity by the age of 3 months. (**D**) Photograph of a dissected lens from a *Vps13b*$^{\Delta Ex3/\Delta Ex3}$ eye in which the cataract had become hypermature. The lens nuclear region was found dissociated from its cortical region. (**E**) In the hypermature stage of cataract, the lens nuclear fragment was sometimes present in the anterior chamber (*arrow*).

Vps13b$^{\Delta Ex3/\Delta Ex3}$ eyes with HC presented with retinal folds and edemas (Fig. 4A, right panel). We therefore assessed the activation of glial cells in retinas by performing GFAP immunostaining. We found, in the vicinity of fibrotic areas of the vitreous humor of eyes with HC, large areas with increased number of GFAP^{+} cells in the ganglion cell layer (GCL) (Fig. 4B, right panels), suggesting that astroglial cells proliferated when the cataract had become hypermature. In addition, low-intensity staining restricted to retinal folds of eyes with HC was reminiscent of immunopositive Müller cells. Immunostaining against the microglial marker Iba1 performed on *Vps13b*$^{\Delta Ex3/\Delta Ex3}$ retinas with HC revealed a higher number of Iba1^{+} cells than in control retinas (Fig. 4C, right panels). The presence of these microglial cells was particularly prominent in the inner and outer plexiform layers, especially where folds and edemas formed. Of note, prior to developing HCs, retinas of 3-month-old *Vps13b*$^{\Delta Ex3/\Delta Ex3}$ mice did not show any glial activation on examined sections.

Western blot analysis (Figs. 5A–5C) revealed an increase in the global retinal content of Iba1 and GFAP on protein extracts from *Vps13b*$^{\Delta Ex3/\Delta Ex3}$ retinas of eyes with HC and to lower extents in some *Vps13b*$^{\Delta Ex3/\Delta Ex3}$ retinas of eyes with non-hypermature cataracts and without cataract. In eyes with HC, the increase in glial content was associated to increased Stat3 expression (Fig. 5D) combined with increased Stat3 and Erk1/2 phosphorylation levels (Figs. 5E, 5F). To a lesser degree, some retinas of *Vps13b*$^{\Delta Ex3/\Delta Ex3}$ eyes without HC also presented with increased Stat3 expression but not Erk1/2 phosphorylation (Figs. 5E, 5F). Overall, these results show that inflammatory events and glial proliferation occur in *Vps13b*$^{\Delta Ex3/\Delta Ex3}$ retinas before cataract onset and through mechanisms that are independent of the cataract. Also, additional inflammation and proliferation occurred upon HC development. A general observation of 6-month-old mice showed the presence of eye discharge, suggesting that a global ocular inflammation was triggered by HC in *Vps13b*$^{\Delta Ex3/\Delta Ex3}$ eyes.

Peculiar Cataract Characteristics in CS Patients

In most forms of pigmented retinopathy, cataract is considered a complication of the retinal degeneration.[29,30]

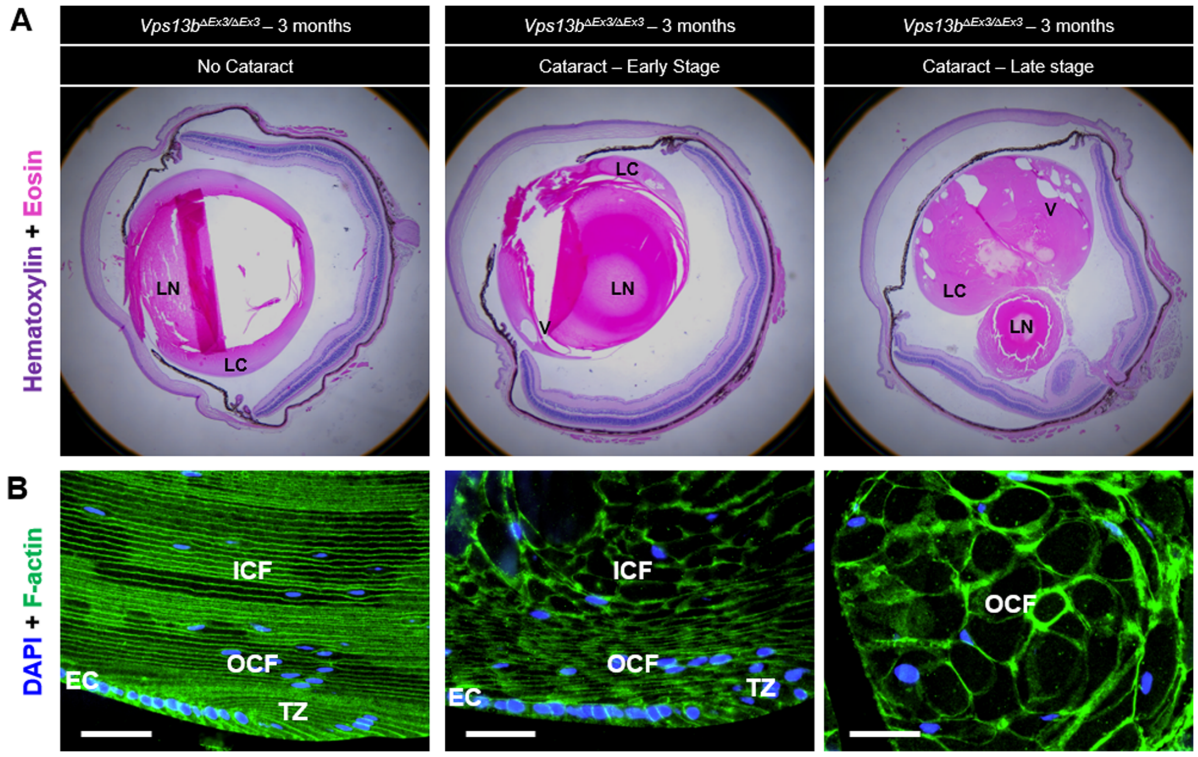

Figure 2. Lens histology of *Vps13b*$^{\Delta Ex3/\Delta Ex3}$ mice compared to controls. (**A**) H&E staining of *Vps13b*$^{\Delta Ex3/\Delta Ex3}$ paraffin eye sections in early-stage (*middle panels*) and late-stage (*lower panels*) cataracts. (**B**) Representative images of immunostaining against F-actin showing lens fiber cell structure after cataract onset in *Vps13b*$^{\Delta Ex3/\Delta Ex3}$ eyes (*middle* and *lower panels*) compared to unaffected *Vps13b*$^{\Delta Ex3/\Delta Ex3}$ eyes (*upper panel*). When cataract occurred, lens fiber cells lost their elongated structure and became enlarged. LN, lens nucleus; LC, lens cortex; V, vacuole; EC, epithelial cells; TZ, transitional zone; OCF, outer cortical fiber cells; ICF, inner cortical fiber cells. *Scale bars*: 10 µm.

Our ophthalmic findings in mice suggest that cataract development in CS may be independent from retinal degenerative processes, as cataract is anterior to most retinopathic features in *Vps13b*$^{\Delta Ex3/\Delta Ex3}$ mice. To assess whether there are specificities to cataract onset in CS patients that differ from other forms of RP-related cataracts, we performed a comprehensive literature analysis of ophthalmic investigations conducted in CS patients (Supplementary Table S1). We found that a third of teenage CS patients were affected with cataract, and the prevalence reached 85% by the age of 40 (Fig. 6A). In contrast, in RP cases, the prevalence of cataract reached only 57%[31] (Fig. 6B). In a comprehensive review on cataracts in RP patients,[31] Pruett reported that most cataracts belong to the posterior subcapsular subtype (80.8%) or a composite form of nuclear sclerosis and posterior subcapsular cataract (12.8%). In contrast, CS patients are mostly affected with nuclear sclerosis (80%), a form of cataract that affects only 6.4% of RP patients (Fig. 6C). Altogether, these observations suggest a mechanism for cataract development that is independent of the pigmented retinopathy in CS.

Complication-Free Cataract Surgery in Two CS Siblings

Two French CS sisters diagnosed with bilateral cataracts in their 40s were operated on at the ages of 48 and 50 years. Postoperative OCT examinations revealed no CME development and best-corrected visual acuity remained stable.

Genotype–Phenotype Correlation and Influence of the Genetic Background on the Onset of Cataract

The high prevalence of nuclear sclerotic cataracts in CS, as well as our findings in mice, suggest a specific function of VPS13B in lens homeostasis. Based on this assumption, we wanted to determine whether some domains or isoforms of VPS13B are more important to lens homeostasis in humans. To date, nothing is known about the functional relevance of the short VPS13B isoforms (NM_181661 and NM_015243), but we suspect that they may carry yet unknown specific functions in a subset of tissues affected in CS, including the ocular lens. We performed an exhaustive bibliographic search of cataracts reported in CS patients with identified disease-causing mutations (Supplementary Table S1). In the Greek CS cohort, which carried a large deletion in the N-terminal region present in NM_181661 and NM_015243, all 12 patients who were 13 years of age and older suffered from cataract. In contrast, in patients with a French ancestry, only one patient developed cataract before their 40s. In contrast with the Greek cohort, they all had in common that they were not affected in a biallelic manner by variants targeting the short N-terminal VPS13B isoforms. This first observation pointed toward either a function of those short N-terminal isoforms in lens homeostasis or an effect of genetic background on the development of cataract (Figs. 6D, 6E). However, when studying the Finnish and Amish cohorts, whose variants did not affect transcripts NM_181661 and NM_015243, we still found a high prevalence of cataracts in teenage and young adult

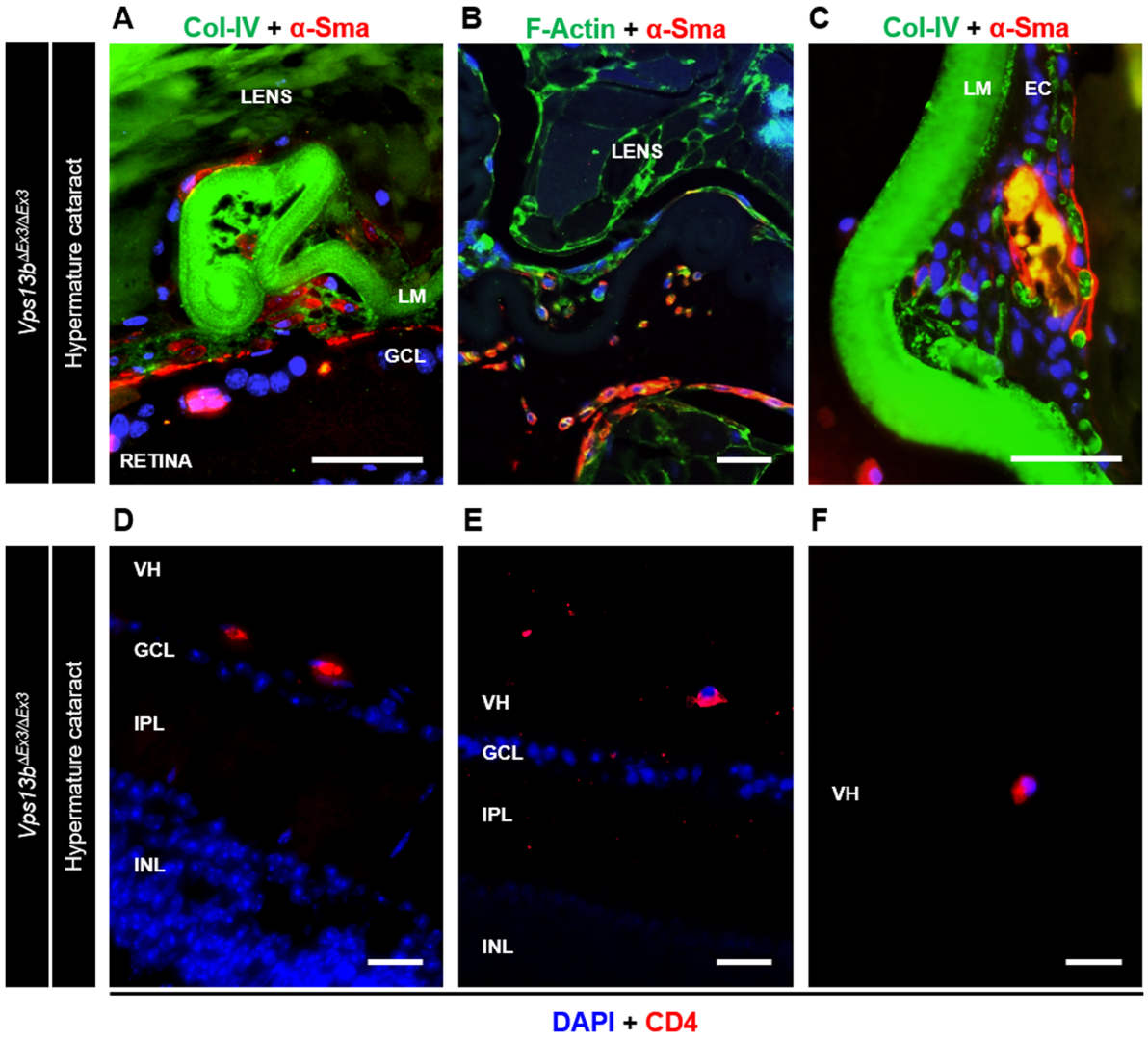

Figure 3. Inflammatory events in cataractous *Vps13b*$^{\Delta Ex3/\Delta Ex3}$ eyes. (**A–C**) Representative images of immunostaining against α-SMA and Col-IV or F-actin ($n = 3$), respectively, targeting mesenchymal cells, their fibrotic secretions, and fiber cell boundaries in the posterior (**A**, **B**) and anterior (**C**) regions of the lens. HC led to EMT and fibrosis at the site of lens envelop rupture and at the anterior pole in *Vps13b*$^{\Delta Ex3/\Delta Ex3}$ eyes. (**D–F**) Images of CD4 immunostaining revealed lymphocyte infiltration in the vitreous humor of *Vps13b*$^{\Delta Ex3/\Delta Ex3}$ eyes with HC ($n = 3$). INL, inner nuclear layer; IPL, inner plexiform layer; GCL, ganglion cell layer; LM, lens membrane; VH, vitreous humor. *Scale bars*: 10 µm.

patients (Supplementary Table S1; Figs. 6D, 6E). In addition, there was a low incidence of cataract in patients with various *VPS13B* variants of French and Asian ancestries of the same age group (Fig. 6D). Therefore, the onset of cataract in CS seems to depend more on modifier effects coming from the genetic background than on the disruption of a lens-specific function present in the short isoforms. In terms of protein domains, all variants associated with early-onset cataract have in common a loss of the VPS13_C and ATG_C domains of the protein; however, those two domains are almost always deleted in CS patients, even those with no cataract in late adulthood.

Selective Breeding and Isolation of a Subline Not Affected with Early-Onset Cataract

Based on the hypothesis that additional genetic factors modify the onset of cataract associated with *Vps13b* variants, we attempted to delineate a cataract-free subline within the *Vps13b*$^{\Delta Ex3/\Delta Ex3}$ mouse line or at least one that is not affected with an early-onset cataract form (i.e., prior to 3 months of age). Through selective breeding of cataract-free 3-month-old *Vps13b*$^{\Delta Ex3/\Delta Ex3}$ females with heterozygous males from litters that showed only cataract-free knockout mice at 3 months of age, we successfully produced a knockout offspring devoid of early-onset cataract. We thereby delineated a cataract-free subline, named hereafter *Vps13b/NC*$^{\Delta Ex3/\Delta Ex3}$. The genealogy related to this subline is presented in Figure 7. In the meantime, random breeding of the general *Vps13b*$^{\Delta Ex3/\Delta Ex3}$ line kept producing a knockout offspring with a high incidence of cataracts (Supplementary Fig. S2), thereby excluding potential changes in the housing conditions as being responsible for the absence of cataract in the *Vps13b/NC*$^{\Delta Ex3/\Delta Ex3}$ subline.

Defining whether this subline is affected by a late-onset form of cataract only or whether the incidence is

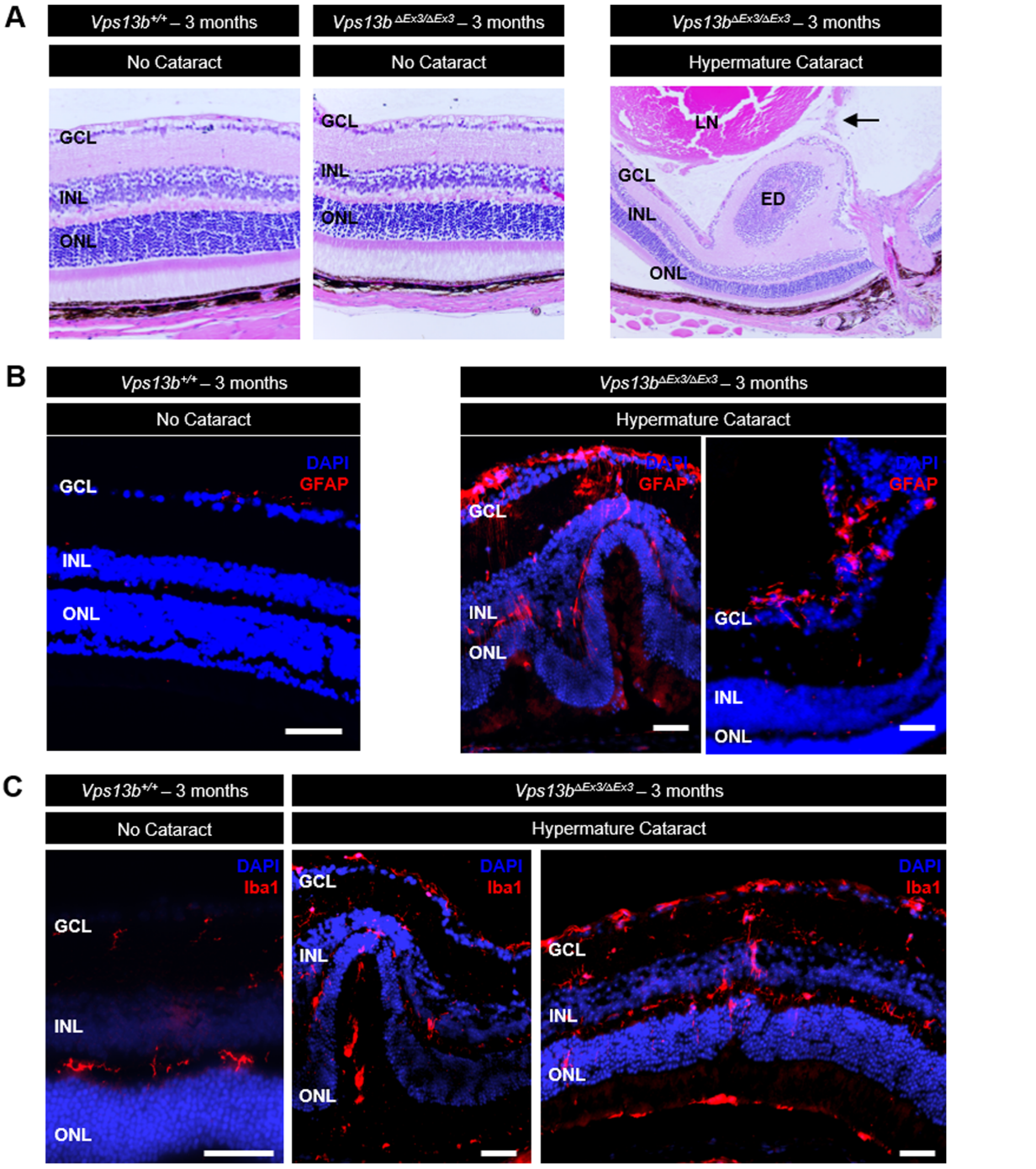

Figure 4. Glial activation in retinas of *Vps13b*$^{\Delta Ex3/\Delta Ex3}$ eyes with and without cataract. (**A–D**) Representative images of retinal sections ($n = 3$ per group) from *Vps13b*$^{+/+}$ eyes (*left panels*) and *Vps13b*$^{\Delta Ex3/\Delta Ex3}$ eyes with hypermature cataract (*right panels*) at 3 months of age stained with H&E (**A**) or antibodies against GFAP (**B**) or Iba1 (**C**). Cataractous eyes (HC) showed large and multiple regions with retinal folds and edemas in which astroglial and microglial proliferations were prominent along with activated Müller cells. The arrow in **A** (*lower panel*) highlights a fibrotic area in the vitreous humor near an edema. VH, vitreous humor; GCL, ganglion cell layer; INL, inner nuclear layer; ONL, outer nuclear layer; ED, edema. *Scale bars*: 10 µm.

also reduced will require additional observations. At the time of writing, three knockout females were kept up to a year of age. Although two of them were still free of cataract, one had developed unilateral cataract at the age of 6 months. At 1 year, the opposite eye remained unaffected.

Discussion

Patients with CS present with a very early-onset form of rod-dominant dystrophy associated with macular changes.[18,23,32,33] Retinal dystrophy occurs in the first years of life and progresses rapidly to a complete loss

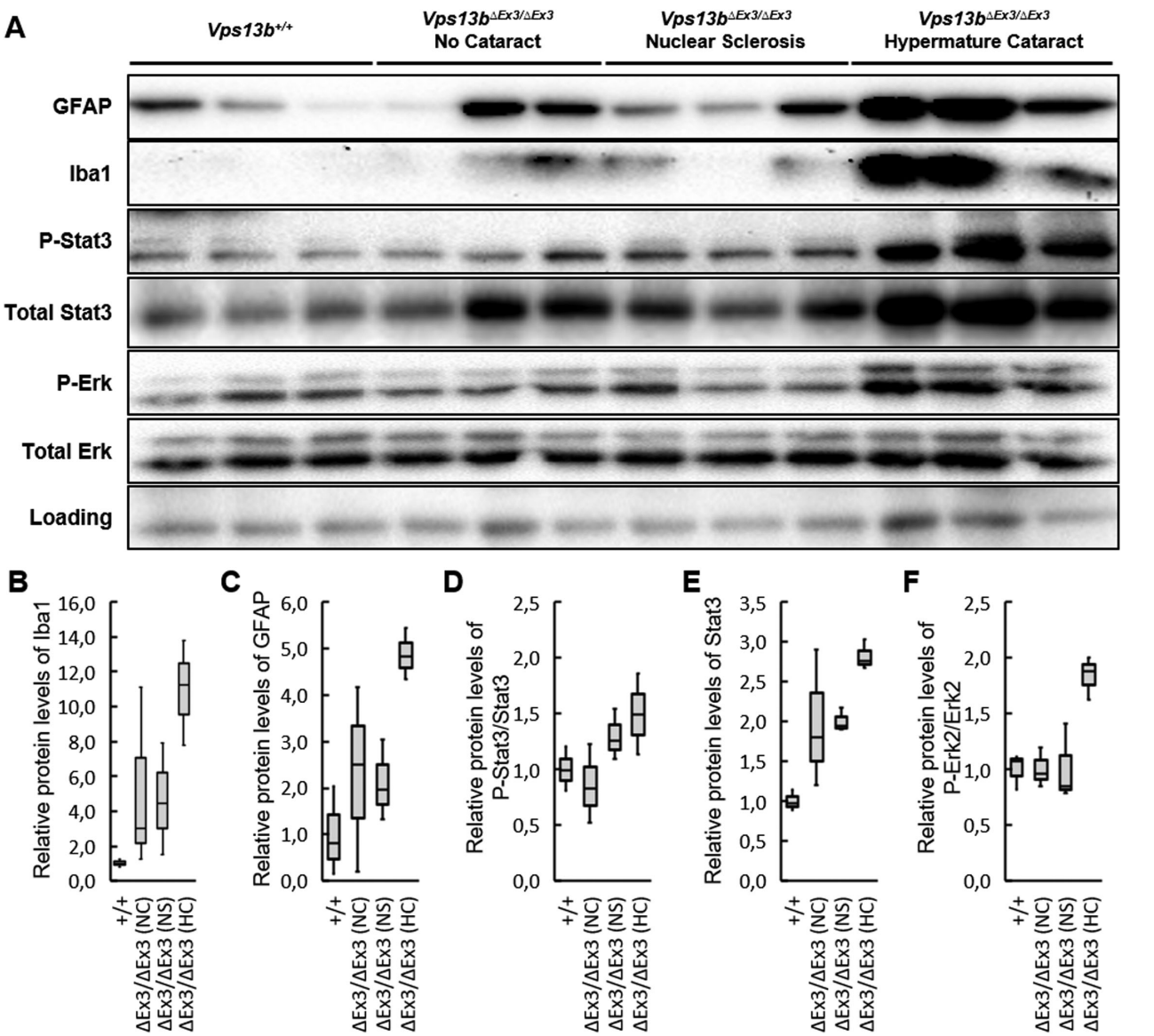

Figure 5. Inflammatory and proliferative profiles of *Vps13b*$^{\Delta Ex3/\Delta Ex3}$ retinas based on protein expression levels. (**A**) Western blot analysis of Iba1 and GFAP expression levels, as well as Stat3 and Erk1/2 phosphorylation levels, on protein extracts from *Vps13b*$^{+/+}$, cataract-free *Vps13b*$^{\Delta Ex3/\Delta Ex3}$, and nuclear sclerotic *Vps13b*$^{\Delta Ex3/\Delta Ex3}$ eyes, as well as *Vps13b*$^{\Delta Ex3/\Delta Ex3}$ eyes with HC, at 2 months of age. GAPDH was used as loading control. (**B**–**F**) Relative protein levels of Iba1, GFAP, Stat3, Phospho-Stat3/Stat3, and Phospho-Erk2/Erk2 from western blot analysis presented in (**A**). Protein levels were normalized to GAPDH levels and the average *Vps13b*$^{+/+}$ value. The data are presented as a boxplot showing minimum, maximum, and quartile values for each group ($n = 3$). Although some *Vps13b*$^{\Delta Ex3/\Delta Ex3}$ retinas of eyes without HC presented with increased Iba1 and GFAP levels representative of glial activation and proliferation, this increase became systematic in eyes with HC. Iba1 was increased by 11-fold (**B**) and GFAP by 5-fold (**C**) compared to controls. In addition, the pro-inflammatory protein Stat3 was also more prominent in retinas of eyes with HC. Comparison of the Phospho-Stat3/Stat3 ratio (**D**) and Stat3/GAPDH ratio (**E**) shows that increased levels of Phospho-Stat3 in cases of HC were mostly due to the overexpression of Stat3. Interestingly, *Vps13b*$^{\Delta Ex3/\Delta Ex3}$ retinas of eyes without HC also displayed a moderately elevated expression of Stat3 that did not translate into increased phosphorylation of the protein. Last, the key regulator of cell proliferation Erk was only over-activated in eyes with HC (**F**).

of peripheral and scotopic vision.[15,16,34] Teenage and young-adult CS patients can also be affected by early-onset cataract.[17] Together with myopia, retinal dystrophy and cataract constitute the major ophthalmic features of CS. To better describe the events associated with those symptoms, characterize their molecular pathomechanisms, and assess potential therapeutic strategies, animal models are required. A canine model with a frameshift deletion in *VPS13B* has been reported.[35] Unfortunately, however, ophthalmic examination of the model was not performed, and the dog breed is now no longer available. We recently reported creation of the *Vps13b*$^{\Delta Ex3/\Delta Ex3}$ mouse model and showed that it displays a defective spermiogenesis due to impaired vesicular transport.[26] In the present study, we showed that *Vps13b*$^{\Delta Ex3/\Delta Ex3}$ mice are affected with cataract prior to retinal changes observed in relation to the rod-dominant CS dystrophy. This is in contrast with the chronology of appearance of these features in CS patients. Together with cataractous characteristics in patients, this finding suggests that cataract in CS may not be secondary to

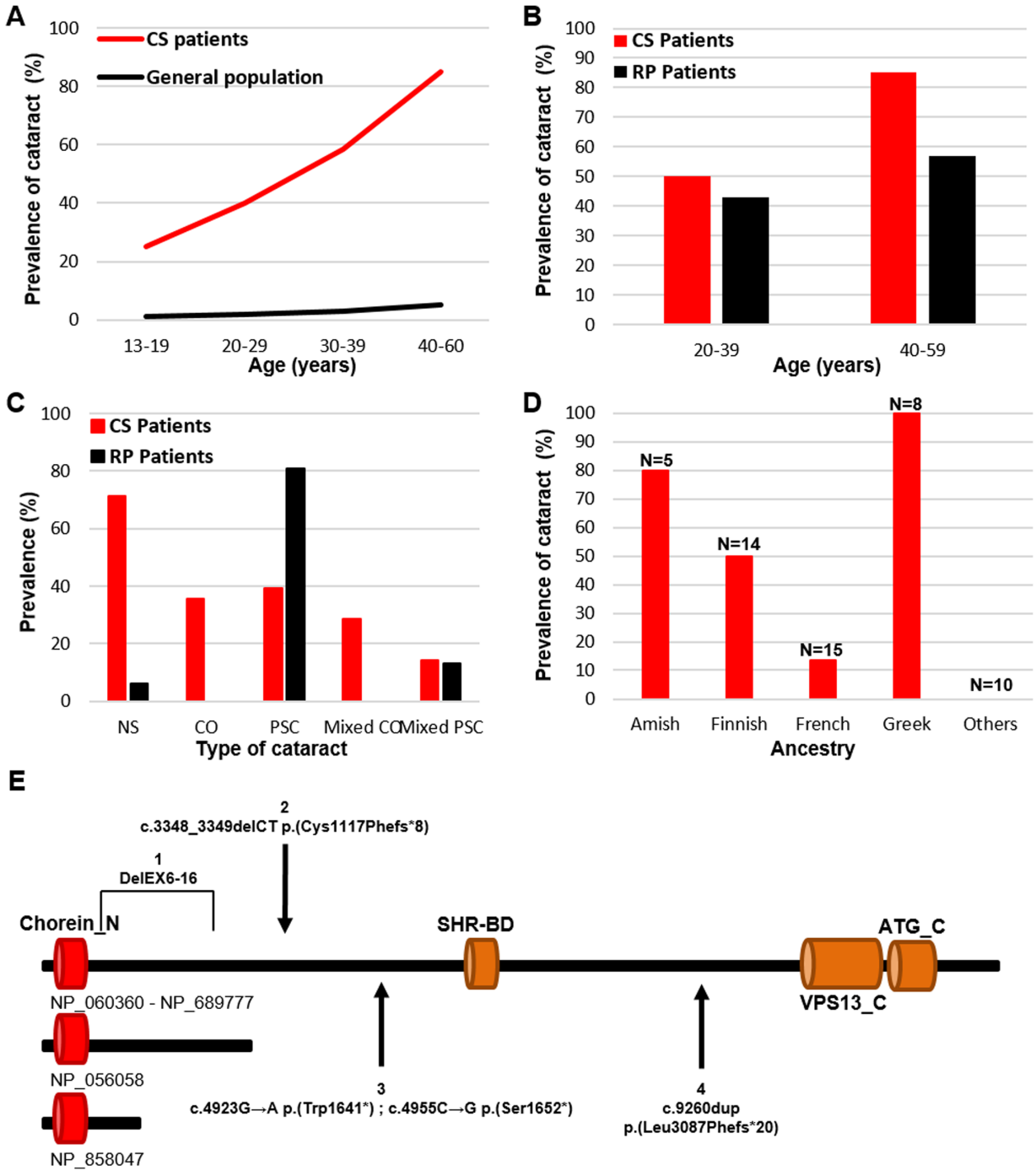

Figure 6. Prevalence of cataract in the CS population. (**A**) Although less than 5% of people in the general population are affected with cataract before the age of 40, the prevalence of cataract in teenage CS patients is around 25%. The prevalence reaches 40% in the 20 to 29 years age group, 58% in the 30 to 39 years age group, and 85% in the age group above 40 years of age. (**B**) Comparison of the prevalence of cataract in CS patients with the data reported by Pruett[31] for RP patients. Compared with RP patients, the prevalence was 7% higher in CS patients from 20 to 39 years of age, and 28% higher in CS patients from 40 to 59 years of age. (**C**) Comparison of the prevalence of each type of cataract between CS and RP patients: nuclear sclerosis (NS), cortical (CO), and posterior polar subcapsular (PSC). CS patients are mostly affected with NS cataracts, whereas RP patients are mostly affected with PSC cataracts. (**D**) Prevalence of cataract in 13- to 40-year-old CS patients depending on their ancestry suggests an effect of the genetic background on the onset of cataract. Greek patients in this age group systematically presented with cataract. Amish and Finnish patients presented with a high prevalence of cataract of about 80% and 50%, respectively. In contrast, the prevalence in patients with French ancestry was lower (13%), and patients with Asian ancestry were never reported with cataract. (**E**) Positions of known *VPS13B* variants associated with cataract in teenage CS patients. As almost systematically reported in CS patients, those variants result in a truncated protein. Numbers 1, 2, and 4 are homozygous variants. Number 3 is a case of two heterozygous variants within the vicinity of one another. No specific domain or isoform of *VPS13B* seems to be associated with teenage onset of cataract in CS. Other truncating variants with similar effect on the loss of protein domain do not cause early-onset cataract (Supplementary Table S1). Chorein_N, N-terminal chorein domain (Pfam 12624); SHR-BD, SHR binding domain of vacuolar protein sorting-associated protein 13 (Pfam 06650); VPS13_C, vacuolar protein sorting-associated protein 13 C-terminal domain (Pfam 16909); ATG_C, autophagy-related protein C-terminal domain (Pfam 09333).

Investigative Ophthalmology & Visual Science

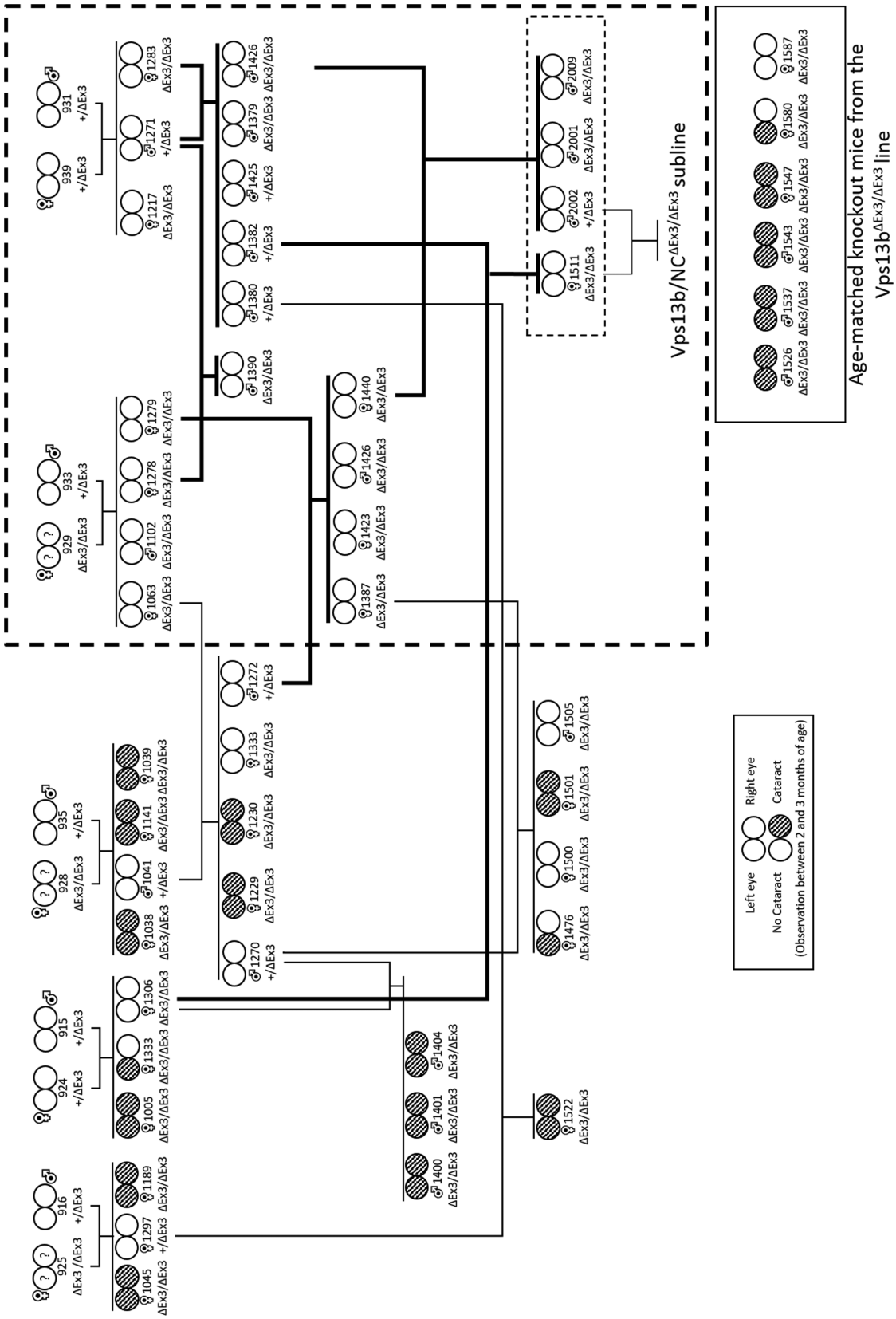

Figure 7. Selective breeding and isolation of the cataract-free *Vps13b/NC*$^{\Delta Ex3/\Delta Ex3}$ subline. In this genealogy, only knockout mice and heterozygous breeders are presented. In addition, all litters from a same mating are depicted under a single line. Cataract-free knockout female mice (ID: 1278, 1283) were crossed with a heterozygous male littermate (ID: 1271) and produced cataract-free offspring (ID: 1390, 1379, 1426). Others (ID: 1063, 1279, 1306, 1387) were crossed with heterozygous males from litters in which cataractous knockout mice were detected (ID: 1041, 1270, 1272) and yielded cataractous knockouts (ID: 1229, 1230, 1400, 1401, 1404, 1476) from males 1041 and 1270

and cataract-free knockouts (ID: 1387, 1423, 1426, 1440) from male 1272. Therefore, transmission of the cataractous trait appeared to be associated with some heterozygous males only. To establish the cataract-free *Vps13b/NC*$^{\Delta Ex3/\Delta Ex3}$ subline we bred a cataract-free knockout female (ID: 1511) with a heterozygous male of a litter that did not display any cataracts among knockouts (ID: 2002).

retinal dystrophy but may arise due to specific defects in lens homeostasis. Expression data from the Affymetrix GeneChip Mouse Genome 430 2.0 array, available at the lens expression resource tool iSyTE (https://research.bioinformatics.udel.edu/iSyTE/ppi/expression.php), also suggests a role for Vps13b in lens development and/or homeostasis, as it is highly expressed during embryonic and postnatal stages in mice. RNA-seq lens enrichment datasets[36] also available at iSyTE shows enrichment of Vps13b at E14.5 and E16.5, embryonic stages of secondary fiber cell differentiation.

Cataracts in *Vps13b*$^{\Delta Ex3/\Delta Ex3}$ mice appeared in most cases between 2 and 3 months of age and rapidly evolved toward a complete dissociation of the cortical and nuclear parts of the lens. In CS patients, cataracts usually appear one to several decades after the onset of retinal dystrophy.[15,17,37] Differences between mouse and human retinal structures, as well as in environmental conditions, might explain the milder effect of Vps13b loss of function on the mouse retina and delayed onset of RD compared to patients. It could also be that the lens-related functions of Vps13b are much more crucial in mice than in humans, explaining the much more precocious onset of cataract in mice.

Recent studies have pointed toward a role for VPS13B in endolysosomal trafficking and autophagy.[26,38,39] The autophagy and lysosome systems have been shown to be essential to maintaining lens transparency in mice.[40,41] Lack of Vps13b has also been associated with protein glycosylation defects,[42] and several congenital forms of cataract are due to variants of genes involved in protein glycosylation.[43–46] In addition, non-enzymatic glycation of crystallins, key structural proteins of the lens, has been shown to be associated with senile and diabetic cataracts.[47] Future studies will aim at identifying whether p62 and ubiquitin-positive aggregates accumulate in lens fiber cells of *Vps13b*$^{\Delta Ex3/\Delta Ex3}$ mice and whether glycosylation of crystallins, as well as structural proteins with numerous or complex glycans, is affected in this model.

During our study, the creation and behavioral analysis of another mouse model for CS (*Vps13b*$^{2-/-}$) was reported by Kim et al.[48] Interestingly, they reported having found no sign of retinal dystrophy and did not mention the presence of cataract in their model, in spite of its being on the C57Bl/6N background, which is susceptible to both retinal and lens alterations.[27,49] However, no information on the ophthalmic examinations they performed is provided in the article. A more thorough report of their investigation would be necessary to comprehend the differences between our models. Our model was created through Cre/LoxP deletion of the third coding exon to introduce multiple stop codons through a frame shift of the coding sequence. Kim et al.[48] deleted the start codon in *Vps13b* exon 2 using the CRISPR/Cas9 system while preserving its reading frame. *Vps13b*$^{2-/-}$ mice still expressed the *Vps13b* mRNA in the hippocampus, and we found in the present study that Vps13b expression was also preserved in the lens of *Vps13b*$^{\Delta Ex3/\Delta Ex3}$ mice (Supplementary Fig. S3). A possible explanation for the ophthalmic differences between our models may be that, in *Vps13b*$^{2-/-}$ mice, a subsequent start codon in exon 3 initiates a Vps13b protein with a shorter N-terminus that is still functional enough to promote Vps13b-related ophthalmic but not all cerebral functions.

Through a retrospective literature analysis of CS case reports and ophthalmic studies, we found that there likely is no correlation between *VPS13B* mutation positions and the onset of cataract, but additional factors in the genetic background of CS patients may contribute to this onset. This observation was substantiated by our ability to isolate the *Vps13b/NC*$^{\Delta Ex3/\Delta Ex3}$ mouse line, which presents delayed cataract onset and/or low cataract incidence on a mixed C57Bl/6N – C57Bl/6J background.

Vps13b$^{\Delta Ex3/\Delta Ex3}$ mice show signs of cataract-induced retinal inflammation. Due to this inflammation, *Vps13b*$^{\Delta Ex3/\Delta Ex3}$ retinas are affected by changes that do not correspond to the retinal dystrophy occurring in CS patients. Future studies will explore whether the *Vps13b/NC*$^{\Delta Ex3/\Delta Ex3}$ subline with late-onset and/or low cataract incidence that we isolated presents with retinal dystrophy before the development of cataract during aging. Nevertheless, identifying the functions of Vps13b in the retina may require the production of conditional models targeting specifically retinal cells to prevent unrelated cataract-induced retinal changes. Considering that additional genetic factors likely contribute to the development of cataract in our model, backcross on a different genetic background could also be considered.

Considering the pace of progression from the initial lens opacification to severe uveitis in *Vps13b*$^{\Delta Ex3/\Delta Ex3}$ mice, CS patients are at high risk of complications if their cataracts are left untreated. New recommendation for CS should thus include a yearly slit-lamp examination to detect cataract formation at an early stage. Cataract surgery is advised to improve visual acuity by clearing the central visual field and to protect the retina from potential cataract-induced uveitis. Cataract surgery on two CS siblings in their 40s did not induce CME and should encourage ophthalmologists to consider cataract surgery in CS cases.

Acknowledgments

The authors thank Christine Arnould and Elodie Noirot from the DImaCell Core Facility (Université de Bourgogne Franche-Comté, Dijon, France) for their technical support; the DImaCell Core Facility is supported by the Regional Council of Bourgogne-Franche Comté. The authors gratefully thank the people from the animal facility of Centre des Sciences du Goût et de l'Alimentation (INRA, Dijon, France) for their care of the animals.

This work, from the FHU-TRANSLAD, is part of the Mascot DM Project (2019) and is supported by the Conseil Régional de Bourgogne and the European Union through the Plan d'Actions Régional pour l'Innovation (PARI) and the Programme opérationnel FEDER-FSE Bourgogne 2014–2020. This work was also supported by funds from the Fondation de France/Fondation de l'Oeil (N.A.) and funds from the JED Fondation (L.F., V.L.). The mouse knockout line was established at the Mouse Clinical Institute (Institut Clinique de la Souris) in the Genetic Engineering

and Model Validation Department with funds from Fondation Maladies Rares.

Disclosure: **V. Lhussiez,** None; **E. Dubus,** None; **Q. Cesar,** None; **N. Acar,** None; **E.F. Nandrot,** None; **M. Simonutti,** None; **I. Audo,** None; **E. Lizé,** None; **S. Nguyen,** None; **A. Geissler,** None; **A. Bouchot,** None; **M. Ansar,** None; **S. Picaud,** None; **C. Thauvin-Robinet,** None; **L. Olivier-Faivre,** None; **L. Duplomb,** None; **R. Da Costa,** None

References

1. Cohen MM, Hall BD, Smith DW, Graham CB, Lampert KJ. A new syndrome with hypotonia, obesity, mental deficiency, and facial, oral, ocular, and limb anomalies. *J Pediatr*. 1973;83:280–284.
2. Kolehmainen J, Black GCM, Saarinen A, et al. Cohen syndrome is caused by mutations in a novel gene, COH1, encoding a transmembrane protein with a presumed role in vesicle-mediated sorting and intracellular protein transport. *Am J Hum Genet*. 2003;72:1359–1369.
3. Seifert W, Holder-Espinasse M, Kühnisch J, et al. Expanded mutational spectrum in Cohen syndrome, tissue expression, and transcript variants of COH1. *Hum Mutat*. 2009;30:E404–E420.
4. Balikova I, Lehesjoki A-E, de Ravel TJL, et al. Deletions in the VPS13B (COH1) gene as a cause of Cohen syndrome. *Hum Mutat*. 2009;30:E845–E854.
5. Chehadeh-Djebbar SE, Faivre L, Moncla A, et al. The power of high-resolution non-targeted array-CGH in identifying intragenic rearrangements responsible for Cohen syndrome. *J Med Genet*. 2011;48:e1.
6. Chandler KE, Kidd A, Al-Gazali L, et al. Diagnostic criteria, clinical characteristics, and natural history of Cohen syndrome. *J Med Genet*. 2003;40:233–241.
7. Kolehmainen J, Wilkinson R, Lehesjoki A-E, et al. Delineation of Cohen syndrome following a large-scale genotype-phenotype screen. *Am J Hum Genet*. 2004;75:122–127.
8. Douzgou S, Petersen MB. Clinical variability of genetic isolates of Cohen syndrome. *Clin Genet*. 2011;79:501–506.
9. Ionita-Laza I, Capanu M, De Rubeis S, McCallum K, Buxbaum JD. Identification of rare causal variants in sequence-based studies: methods and applications to VPS13B, a gene involved in Cohen syndrome and autism. *PLoS Genet*. 2014;10:e1004729.
10. Gueneau L, Duplomb L, Sarda P, et al. Congenital neutropenia with retinopathy, a new phenotype without intellectual deficiency or obesity secondary to VPS13B mutations. *Am J Med Genet A*. 2014;164A:522–527.
11. Rafiq MA, Leblond CS, Saqib MAN, et al. Novel VPS13B mutations in three large Pakistani Cohen syndrome families suggests a Baloch variant with autistic-like features. *BMC Med Genet*. 2015;16:41.
12. El Chehadeh S, Aral B, Gigot N, et al. Search for the best indicators for the presence of a VPS13B gene mutation and confirmation of diagnostic criteria in a series of 34 patients genotyped for suspected Cohen syndrome. *J Med Genet*. 2010;47:549–553.
13. El Chehadeh-Djebbar S, Blair E, Holder-Espinasse M, et al. Changing facial phenotype in Cohen syndrome: towards clues for an earlier diagnosis. *Eur J Hum Genet*. 2013;21:736–742.
14. Seifert W, Holder-Espinasse M, Spranger S, et al. Mutational spectrum of COH1 and clinical heterogeneity in Cohen syndrome. *J Med Genet*. 2006;43:e22.
15. Kivitie-Kallio S, Summanen P, Raitta C, Norio R. Ophthalmologic findings in Cohen syndrome. A long-term follow-up. *Ophthalmology*. 2000;107:1737–1745.
16. Chandler KE, Biswas S, Lloyd IC, Parry N, Clayton-Smith J, Black GCM. The ophthalmic findings in Cohen syndrome. *Br J Ophthalmol*. 2002;86:1395–1398.
17. Douzgou S, Samples JR, Georgoudi N, Petersen MB. Ophthalmic findings in the Greek isolate of Cohen syndrome. *Am J Med Genet A*. 2011;155A:534–539.
18. Resnick K, Zuckerman J, Cotlier E. Cohen syndrome with bull's eye macular lesion. *Ophthalmic Paediatr Genet*. 1986;7:1–8.
19. Nelson ML, Martidis A. Managing cystoid macular edema after cataract surgery. *Curr Opin Ophthalmol*. 2003;14:39–43.
20. Dikopf MS, Chow CC, Mieler WF, Tu EY. Cataract extraction outcomes and the prevalence of zonular insufficiency in retinitis pigmentosa. *Am J Ophthalmol*. 2013;156:82–88.e2.
21. Davies EC, Pineda R. Cataract surgery outcomes and complications in retinal dystrophy patients. *Can J Ophthalmol*. 2017;52:543–547.
22. Jackson H, Garway-Heath D, Rosen P, Bird AC, Tuft SJ. Outcome of cataract surgery in patients with retinitis pigmentosa. *Br J Ophthalmol*. 2001;85:936–938.
23. Uyhazi KE, Binenbaum G, Carducci N, Zackai EH, Aleman TS. Early photoreceptor outer segment loss and retinoschisis in Cohen syndrome. *Ophthalmic Genet*. 2018;39:399–404.
24. Beck KD, Wong RW, Gibson JB, Harper CA. Nonleaking cystoid macular edema in Cohen syndrome. *J AAPOS*. 2019;23:38–39.e1.
25. Nasser F, Kurtenbach A, Biskup S, Weidensee S, Kohl S, Zrenner E. Ophthalmic features of retinitis pigmentosa in Cohen syndrome caused by pathogenic variants in the VPS13B gene. *Acta Ophthalmol*. 2020;98:e316–e321.
26. Da Costa R, Bordessoules M, Guilleman M, et al. Vps13b is required for acrosome biogenesis through functions in Golgi dynamic and membrane trafficking. *Cell Mol Life Sci*. 2020;77:511–529.
27. Mattapallil MJ, Wawrousek EF, Chan C-C, et al. The Rd8 mutation of the Crb1 gene is present in vendor lines of C57BL/6N mice and embryonic stem cells, and confounds ocular induced mutant phenotypes. *Invest Ophthalmol Vis Sci*. 2012;53:2921–2927.
28. Shirai K, Tanaka S-I, Lovicu FJ, Saika S. The murine lens: a model to investigate in vivo epithelial-mesenchymal transition. *Dev Dyn*. 2018;247:340–345.
29. Fishman GA, Anderson RJ, Lourenco P. Prevalence of posterior subcapsular lens opacities in patients with retinitis pigmentosa. *Br J Ophthalmol*. 1985;69:263–266.
30. Fujiwara K, Ikeda Y, Murakami Y, et al. Risk factors for posterior subcapsular cataract in retinitis pigmentosa. *Invest Ophthalmol Vis Sci*. 2017;58:2534–2537.
31. Pruett RC. Retinitis pigmentosa: clinical observations and correlations. *Trans Am Ophthalmol Soc*. 1983;81:693–735.
32. Beck KD, Wong RW, Gibson JB, Harper CA. Nonleaking cystoid macular edema in Cohen syndrome. *J AAPOS*. 2019;23:38–39.e1.
33. Nasser F, Kurtenbach A, Biskup S, Weidensee S, Kohl S, Zrenner E. Ophthalmic features of retinitis pigmentosa in Cohen syndrome caused by pathogenic variants in the VPS13B gene. *Acta Ophthalmol*. 2020;98:e316–e321.
34. Taban M, Memoracion-Peralta DSA, Wang H, Al-Gazali LI, Traboulsi EI. Cohen syndrome: report of nine cases and review of the literature, with emphasis on ophthalmic features. *J AAPOS*. 2007;11:431–437.
35. Shearman JR, Wilton AN. A canine model of Cohen syndrome: trapped neutrophil syndrome. *BMC Genomics*. 2011;12:258.
36. Anand D, Kakrana A, Siddam AD, Huang H, Saadi I, Lachke SA. RNA-sequencing-based transcriptomic profiles

of embryonic lens development for cataract gene discovery. *Hum Genet*. 2018;137:941–954.

37. Mrugacz M, Sredzinska-Kita D, Bakunowicz-Lazarczyk A. Pediatric ophthalmologic findings of Cohen syndrome in twins. *J Pediatr Ophthalmol Strabismus*. 2005;42: 54–56.
38. Koike S, Jahn R. SNAREs define targeting specificity of trafficking vesicles by combinatorial interaction with tethering factors. *Nat Commun*. 2019;10:1608.
39. Lee Y-K, Lee S-K, Choi S, et al. Autophagy pathway upregulation in a human iPSC-derived neuronal model of Cohen syndrome with VPS13B missense mutations. *Mol Brain*. 2020;13:69.
40. Morishita H, Eguchi S, Kimura H, et al. Deletion of autophagy-related 5 (Atg5) and Pik3c3 genes in the lens causes cataract independent of programmed organelle degradation. *J Biol Chem*. 2013;288:11436–11447.
41. Sidjanin DJ, Park AK, Ronchetti A, Martins J, Jackson WT. TBC1D20 mediates autophagy as a key regulator of autophagosome maturation. *Autophagy*. 2016;12:1759–1775.
42. Duplomb L, Duvet S, Picot D, et al. Cohen syndrome is associated with major glycosylation defects. *Hum Mol Genet*. 2014;23:2391–2399.
43. Thiel C, Schwarz M, Peng J, et al. A new type of congenital disorders of glycosylation (CDG-Ii) provides new insights into the early steps of dolichol-linked oligosaccharide biosynthesis. *J Biol Chem*. 2003;278:22498–22505.
44. Pras E, Raz J, Yahalom V, et al. A nonsense mutation in the glucosaminyl (*N*-acetyl) transferase 2 gene (*GCNT2*): association with autosomal recessive congenital cataracts. *Invest Ophthalmol Vis Sci*. 2004;45:1940–1945.
45. Kahrizi K, Hu CH, Garshasbi M, et al. Next generation sequencing in a family with autosomal recessive Kahrizi syndrome (OMIM 612713) reveals a homozygous frameshift mutation in SRD5A3. *Eur J Hum Genet*. 2011;19:115–117.
46. Lepais L, Cheillan D, Frachon SC, et al. ALG3-CDG: report of two siblings with antenatal features carrying homozygous p.Gly96Arg mutation. *Am J Med Genet A*. 2015;167A:2748–2754.
47. Sharma KK, Santhoshkumar P. Lens aging: effects of crystallins. *Biochim Biophys Acta*. 2009;1790:1095–1108.
48. Kim MJ, Lee RU, Oh J, et al. Spatial learning and motor deficits in vacuolar protein sorting-associated protein 13b (Vps13b) mutant mouse. *Exp Neurobiol*. 2019;28:485–494.
49. Moore BA, Roux MJ, Sebbag L, et al. A population study of common ocular abnormalities in C57BL/6N rd8 mice. *Invest Ophthalmol Vis Sci*. 2018;59:2252–2261.

Investigative Ophthalmology & Visual Science